# Interspecies distances between propionic acid degraders and methanogens in syntrophic consortia for optimal hydrogen transfer

Monika Felchner-Zwirello · Josef Winter · Claudia Gallert

**Abstract** A mixed culture from an anaerobic biowaste digester was enriched on propionate and used to investigate interspecies hydrogen transfer in dependence of spatial distances between propionate degraders and methanogens. From 20.3 mM propionate, 20.8 mM acetate and 15.5 mM methane were formed. Maximum specific propionate oxidation and methane formation rates were 49 and 23 mmol mg$^{-1}$day$^{-1}$, respectively. Propionate oxidation was inhibited by only 20 mM acetate by about 50 %. Intermediate formate formation during inhibited methanogensis was observed. The spatial distribution and the biovolume fraction of propionate degraders and of methanogens in relation to the total population during aggregate formation were determined. Measurements of interbacterial distances were conducted with fluorescence in situ hybridization by application of group-specific 16S rRNA-targeted probes and 3D image analyses. With increasing incubation time, floc formation and growth up to 54 μm were observed. Propionate degraders and methanogens were distributed randomly in the flocs. The methanogenic biovolume fraction was high at the beginning and remained constant over 42 days, whereas the fraction of propionate degraders increased with time during propionate feeding. Interbacterial distances between propionate degraders and methanogens decreased with time from 5.30 to 0.29 μm, causing an increase of the maximum possible hydrogen flux from 1.1 to 10.3 nmol ml$^{-1}$min$^{-1}$. The maximum possible hydrogen flux was always higher than the hydrogen formation and consumption rate, indicating that reducing the interspecies distance by aggregation is advantageous in complex ecosystems.

**Keywords** Propionate degrading enrichment · Interspecies hydrogen transfer · Syntrophy · Cell aggregation · Interspecies distance

M. Felchner-Zwirello · J. Winter · C. Gallert
Institut für Ingenieurbiologie und Biotechnologie des Abwassers,
KIT—Karlsruher Institut für Technologie, Am Fasanengarten,
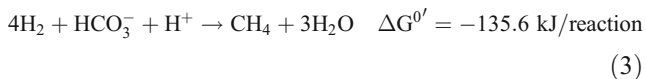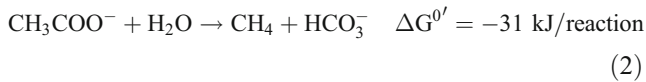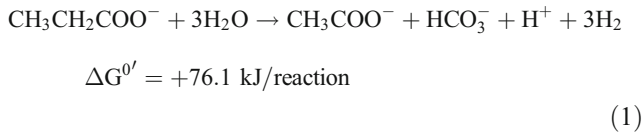76131 Karlsruhe, Germany

M. Felchner-Zwirello
e-mail: Monika.Felchner-Zwirello@kit.edu

J. Winter
e-mail: Josef.Winter@kit.edu

M. Felchner-Zwirello
Department of Analytical Chemistry, Gdańsk University
of Technology, Gabriela Narutowicza 11/12 Str.,
80-233 Gdańsk, Poland

C. Gallert (✉)
FB Technik/Abteilung Mikrobiologie-Biotechnologie,
Hochschule Emden-Leer, Constantiaplatz 4,
26723 Emden, Germany
e-mail: Claudia.Gallert@hs-emden-leer.de

## Introduction

Complex organic matter is degraded in anoxic or anaerobic environment to methane and carbon dioxide by syntrophic interaction of bacteria and archaea. Fermentative bacteria degrade organic substances to volatile fatty acids (VFAs), mainly acetate, propionate, and butyrate or additionally to lactate and ethanol at increasing hydrogen partial pressure. Except for acetate, these intermediates are highly reduced and must be converted by acetogenic bacteria to the methane precursors acetate, formate, or hydrogen (Gujer and Zehnder 1983; Gallert and Winter 2005). Propionate plays a crucial role due to the unfavorable thermodynamics ($\Delta G^{0'}>0$) for its fermentation to acetate, $CO_2$, and hydrogen. Anaerobic cleavage of propionate is possible only if the reaction products hydrogen and also acetate (Eq. 1) were removed effectively by, e.g., methanogens (Eqs. 2 and 3) or sulfate reducers in obligate

syntrophic association with proton-reducing acetogenic bacteria (Schink 1992).

$$CH_3CH_2COO^- + 3H_2O \rightarrow CH_3COO^- + HCO_3^- + H^+ + 3H_2$$

$$\Delta G^{0\prime} = +76.1 \text{ kJ/reaction}$$
(1)

$$CH_3COO^- + H_2O \rightarrow CH_4 + HCO_3^- \quad \Delta G^{0\prime} = -31 \text{ kJ/reaction}$$
(2)

$$4H_2 + HCO_3^- + H^+ \rightarrow CH_4 + 3H_2O \quad \Delta G^{0\prime} = -135.6 \text{ kJ/reaction}$$
(3)

The problem of VFA accumulation, especially of propionate, in anaerobic digesters has been recorded repeatedly (e.g., Inanc et al. 1999; Wang et al. 2006; Gallert and Winter 2008). The thermodynamic disadvantage of propionate degradation (Eq. 1) makes it the substrate, which often persists in anaerobic reactors (Shin et al. 2010). Unfavorable thermodynamic conditions prevail also for n-butyrate ($\Delta G^{0\prime}=+48.1$ kJ). Both VFAs require a very low hydrogen partial pressure for degradation and hence syntrophic partner organisms (Dong and Stams 1995).

Propionate is the "leading" volatile fatty acid during anaerobic digestion, being converted to acetic acid, $CO_2$, and $H_2$ (Gerardi 2003). Two metabolic pathways for anaerobic propionate oxidation were described: In bacteria that express the methyl–malonyl–CoA pathway, propionate is fermented to acetate and $CO_2$ (Plugge et al. 1993) with release of reducing equivalents for oxidation of succinate to fumarate, malate to oxaloacetate, or pyruvate to acetyl–CoA, whereas bacteria that express the C6-dismutation pathway (de Bok et al. 2001) convert 2 mol of propionate to 3 mol of acetate with *n*-butyrate as an intermediate. Hydrogen and/or formate utilization for methane production or sulfate reduction is the driving force of anaerobic propionate oxidation. In anaerobic digesters, coupled methane formation keeps the hydrogen partial pressure pH$_2$ low enough for propionate oxidation (Thauer et al. 1977). The maximal pH$_2$ which still allows anaerobic butyrate or propionate oxidation ($\Delta G^{\prime}<0$) is 186 or 6.5 Pa, respectively at 25 °C, pH of 7, and 1 mM propionate concentration. Therefore, the specific activity of hydrogen-oxidizing methanogens controls favorable bioenergetic conditions for methane formation from organic material (Dwyer et al. 1988). Bryant et al. (1967) and Wolin (1975) called this process interspecies hydrogen transfer, but formate apparently can also be used as a buffer for interspecies electron flow (Thiele and Zeikus 1988; Bleicher and Winter 1994; Stams and Dong 1995). Comparing the diffusion constant and the solubility

of hydrogen and formate, it can be expected from Fick's diffusion law that formate transfer from the producer to the consumer is the favored mechanism when interspecies distances are high, while hydrogen transfer becomes more favorable when interspecies distances are low (de Bok et al. 2004). Recent biochemical studies and genome analyses of pure cultures of syntrophic volatile fatty acid degraders indicated that hydrogen and formate transfer may occur simultaneously (Müller et al. 2010).

Small interspecies distances can be maintained by growth in flocs, granules, or aggregates or by inoculation of additional hydrogen consumers, which leads to increased propionate degradation rates (Dwyer et al. 1988; Thiele et al. 1988; Schmidt and Ahring 1995; Imachi et al. 2000; Ishii et al. 2005). As diffusion is the major process of hydrogen transport between microbial species (McCarty and Smith 1986), it appears from Fick's diffusion law that the hydrogen flux depends, inter alia, on the distance between $H_2$-producing and $H_2$-consuming organisms. The same considerations would be valid for formate flux calculations (Stams 1994). The standard redox potential of the $H^+/H_2$ couple is −414 mV and is almost the same as for the $CO_2$/formate couple (−420 mV). Both electron transfer reactions are important in syntrophic interactions (Schink 1997). Formate formation and degradation governed by the hydrogen partial pressure are of importance for electron transfer in syntrophic cultures. Until now, interspecies distances for an optimal electron transfer have only been calculated theoretically. Applied Fick's diffusion law computations revealed interspecies distances of syntrophic propionate oxidizers from methanogens of less than 3 μm (Schmidt and Ahring 1995), 2 μm (Ishii et al. 2005), 1 μm (Stams et al. 1989; Imachi et al. 2000), or even only 0.08 μm (Shi-yi and Jian 1992).

The aim of our study was to determine the correlation between aggregate growth and resulting interspecies distances of a mixed culture, enriched from a full-scale digester with propionate as the sole carbon source. Oxidation rates of propionate at different stages of growth were balanced with acetate and methane production. Measurements of interspecies distances are reported for the first time and results are discussed in relation to data from literature.

## Materials and methods

### Preparation of an enrichment culture

Liquid samples of a full-scale anaerobic reactor treating a biowaste suspension from source sorted biowaste collection of the City of Karlsruhe, Germany (Gallert et al. 2003), were suspended in a mineral medium (Felchner-Zwirello et al. 2012) with addition of propionate as the sole carbon source. Enrichments on propionate were carried out over a 3-year

period by means of 10 % monthly transfers into fresh medium, resulting in a mixed culture that consisted mainly of non-filamentous hydrogentrophic methane bacteria and lemon-shaped Gram-negative propionate degraders forming aggregates. The enrichment was cultivated in serum bottles that were closed with a rubber stopper and secured with an aluminum cap under a nitrogen gas atmosphere at 37 °C with gentle shaking in darkness. The pH of the mineral medium was 7. Propionic acid (Fluka Germany) from a 1-M stock solution in distilled water was repeatedly fed to give 5 mM starting concentration. After each feeding, the slight drop of the pH was corrected with 0.1 ml NaOH (1 M) to 7. Acetate, $CO_2$, and methane were the main products of the enrichment culture. *Methanosarcina*-like methanogens were originally present in the inoculum from the full-scale digester, forming big aggregates, but these were lost (or diluted out) during 3 years of enrichment.

### Sample preparation and experimental setup

The propionate-degrading enrichment of bacteria was cultured in 250-ml Schott bottles. One hundred ml of mineral medium was inoculated with 10 ml digester effluent or pregrown enrichment culture. Directly after inoculation and every day later on, 1-ml samples were withdrawn for analyses of propionic acid, acetic acid and the protein content (as a measure of cell growth). Methane, carbon dioxide, and hydrogen were withdrawn from the gas phase and determined every day by gas chromatography. Whenever propionic acid was degraded, biomass was collected for fluorescence in situ hybridization (FISH) in order to differentiate between propionate degraders and hydrogenotrophic methane bacteria. Organisms were identified after reaction with 16S rRNA-based oligonucleotide probes specific for *Bacteria*, propionate degraders, and *Archaea* (probe sequences are provided in "Microscopy"). The experiment was divided into five phases, namely, phase 0 (directly after inoculation), growth phase 1 for degradation of the first portion of propionate (until day 13), growth phase 2 after the second propionate feeding (day 22), growth phase 3 after the third propionate feeding (day 29), and growth phase 4 after the fourth propionate feeding (day 42). The experiment was carried out in duplicate and repeated tree times. Since the results of each experiment were similar, only one representative experiment is shown in this paper.

To determine the influence of acetate on propionate oxidation rates, 5, 10, 15, and 20 mM acetate was added together with the propionate feeding to 40-ml assays. Propionate oxidation rates were then determined in the presence of acetate.

Since formate might be an alternative electron carrier during syntrophic propionate degradation, methane generation of the enrichment culture from $H_2/CO_2$ (80:20 %; vol/vol) and formate (15 mM) in non-inhibited and in inhibited assays (by 10 mM bromoethane sulfonic acid, BESA) was compared. Ten-milliliter cultures in 22-ml glass vials (closed with a rubber stopper and sealed with an aluminum cap) were fed with $H_2/CO_2$ (2 atm) or 15 mM formate in the absence of propionate. Methane production in the presence or absence of 10 mM BESA was measured daily and corrected against the blank.

### Analytical measurements

Methane, hydrogen, and carbon dioxide concentrations in the gas phase were analyzed with a Chrompack CP 9001 gas chromatograph (GC) equipped with a 50-m CP-Sil 8CB column (0.32 mm internal diameter (ID)) and a thermal conductivity detector. The detection limit of hydrogen was 128 Pa, which was not sensitive enough to measure hydrogen concentrations during interspecies $H_2$ transfer. Propionate and acetate were measured with a combination of a model 3950-Headspace sampling unit coupled to a Varian 431C GC and a Varian 210 mass spectrometer. A 30-m CP-Wax FFAP column of 0.25 ID was used for VFA separation (Felchner-Zwirello et al. 2012). The precision of measurements (%-RSD) was for acetic acid 6.8 %, for propionic acid 7.4 % and for methane 3 %, expressed as maximal coefficient of variation obtained for the concentration range measured during the experiment.

The protein concentration was measured photometrically with a Hach Lange DR 5000 spectrophotometer according to Lowry et al. (1951) after extraction of protein from single-cell or cell aggregate suspensions with 1 ml 1 M NaOH at 95 °C for 10 min. Triplicate analyses of each parameter for each sample were carried out and mean values were calculated.

Formic acid was quantified with R-Biopharm No. 10979732035 enzymatic assay (Boehringer, Mannheim, Germany). $NADH/H^+$ formation by formate dehydrogenase was determined spectrophotometrically at 340 nm. The detection limit of formate was 1 $mg\,l^{-1}$ corresponding to 0.02 mM.

### Microscopy

Fluorescence in situ hybridization was performed with 16S rRNA-based oligonucleotide probes specific for *Archaea* (Arc915: 5′GTG CTC CCC CGC CAA TTC CT; Stahl and Amann 1991) for most of the *Bacteria* (Eub338: 5′GCT GCC TCC CGT AGG AGT; Amann et al. 1990) and for two propionic acid degraders: MPOB1: 5′ACG CAG GCC CAT CCC CGA A, labeled at the 5′ end with 6-carboxyfluorescein (FAM) for *Syntrophobacter fumaroxidans*-related organisms and KOP1: 5′TCA AGT CCC CAG TCT CTT CGA, labeled with cyanine 3 (Cy3) for *Syntrophobacter pfennigii*-related organisms (Harmsen et al.

1996). The probes were obtained from Eurofins MWG Operon, Ebersberg, Germany. The MPOB1 probe gave a signal for both, MPOB and KOP organisms (Harmsen et al. 1995), so the results might denote the presence of both groups of propionate degraders, whereas KOP1 reacted only with *S. pfennigii*-related organisms. After sample hybridization, 10 μl of biomass suspension was distributed onto each hole of a Teflon-coated microscope slide, air-dried, dehydrated in ethanol, and further processed as described by Amann et al. (1990). Oligonucleotide probes were prepared at a concentration of 5 pmol μl$^{-1}$, and 4 μl of each was spread onto the specimen, together with 8 μl of hybridization buffer with 30 % formamide. Before microscopic observation, counterstaining with 0.1 μM 4,6-diamidino-2-phenylindol (DAPI) on ice for 15 min in darkness was done. Each sample from a certain growth phase (0–4) was prepared in octets and ten representative microscopic images were taken with an ApoTome (Axio Imager Z1, Zeiss, Jena, Germany) per "hole", giving altogether 80 images for further analysis. The epifluorescence microscope with Apo-Tome technique was equipped with several filter sets suitable for the used dyes Cy3, FITC (or FAM), and DAPI.

A series of microphotographs were taken in order to get a 3D aggregate image, with a z-stack dimension set at 0.3 μm. The AxioVision software (Carl Zeiss Micro Imaging GmbH, Jena, Germany) was applied for analysis of obtained microphotographs.

The interspecies distances between differently stained organisms were measured manually with all relevant z-stack images. Measurements had an accuracy of 0.01 μm. For each growth phase, the interspecies distance between MPOB1-hybridized propionate degraders (*S. fumaroxidans*-related organisms) and Arc915-hybridized methanogens in the closest vicinity was measured, requiring three up to 15 measurements per single image. Dispersed bacteria (single cells) were only considered in phase 0 directly after inoculation. During all further growth phases, aggregates were examined. Per growth phase, 80 microscopic images were used for analysis, meaning that 240 up to 1,200 single measurements of interspecies distances were performed to calculate this value. Additionally, the size of the formed aggregates was measured: broadness (*x*), height (*y*), and thickness (*z*). The obtained values were averaged for each image.

Population changes during the different growth phases of the enrichment culture were evaluated with the *daime* software for digital image analysis in microbial ecology (Daims et al. 2006). The same microscopic images as described above were used for biovolume fraction evaluation, relying on the comparison of the total biovolume (biomass stained with unspecific fluorescent dye DAPI) and the biovolume fraction of the bacterial and archaeal population that reacted with 16S rRNA-targeted specific oligonucleotide probes labeled with different fluorescent dyes.

### Interspecies hydrogen transfer versus distances between organisms: hydrogen fluxes

Hydrogen that was released by the propionate-degrading organisms (PA) must be transferred to the hydrogen-consuming methanogens by diffusion. According to Fick's diffusion law (Eq. 4), the hydrogen flux ($J_{H_2}$) depends on the surface area of the H$_2$-producing, propionate-degrading organisms ($A_{PA}$), the hydrogen diffusion constant in water ($D_{H_2}$), the difference of the hydrogen concentration outside the hydrogen producer ($C_{PA}$) and the hydrogen consumer ($C_{H_2}$), and the interspecies distance between the two considered organisms ($d_{PAH_2}$).

$$J_{H_2} = A_{PA} \cdot D_{H_2} \frac{C_{PA} - C_{H_2}}{d_{PAH_2}} \tag{4}$$

The difference of the hydrogen concentration at the cell surface of the hydrogen producer ($C_{PA}$) and the hydrogen consumer ($C_{H_2}$) was calculated according to Eq. 5, giving the maximum allowed H$_2$ concentration for propionate oxidation ($\Delta G < 0$) of 9.34 Pa and the minimum H$_2$ concentration required for methane production ($\Delta G > 0$) of 0.32 Pa. The calculated difference, $C_{PA} - C_{H_2}$, was set as a constant value during the different growth phases since it was not possible to measure hydrogen in the gas or liquid phase with the necessary low detection limit. The calculated H$_2$ flux after measuring the interspecies distances was therefore the "maximum possible H$_2$ flux".

$$\Delta G = \Delta G° + RT \ln K \tag{5}$$

### Statistical analysis

Statistical analysis (one- or two-way ANOVA) and curve fittings were performed with the statistic program Graph Pad Prism 4.0 (GraphPad Software, Inc., USA).

## Results

### Propionate degradation

The propionate-degrading enrichment culture was cultivated for 42 days under mesophilic conditions with four propionate feedings. Degradation of the four portions of propionate during the four growth phases, cumulative acetate and methane production, as well as the increasing protein concentration are shown in Fig. 1. Whenever 5 mM propionate was anaerobically oxidized by the mixed culture, propionate was replenished. The capacity of the carbonate buffer was sufficient to stabilize the pH at 7 during the experiment. pH adjustment with 0.1 ml NaOH (1 M) was only required after

Fig. 1 Syntrophic oxidation of 5-mM portions of propionate by the enrichment culture and formation of acetate and methane during growth. Cell growth was measured as increasing concentration of protein after cell or aggregate harvest and hydrolysis with NaOH
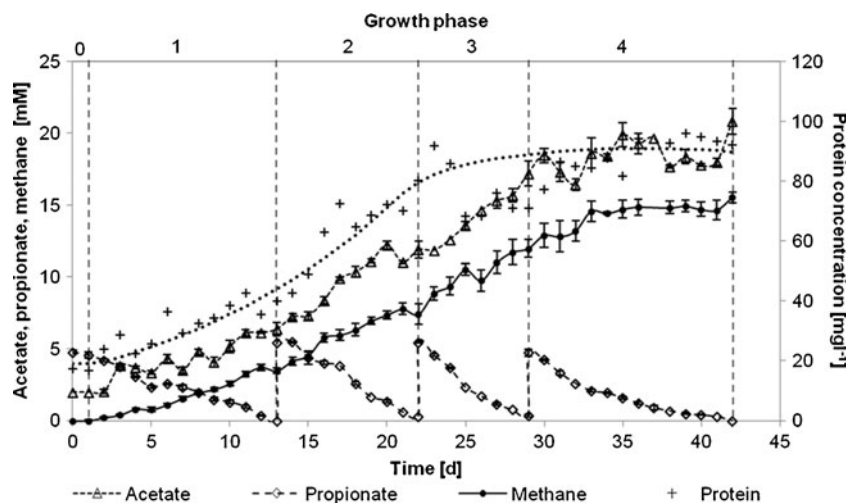


every feeding with propionic acid. According to the stoichiometries depicted in Eqs. (1) and (3), from 1 mol of propionate maximally 1 mol of acetate and 0.75 mol of methane could be produced, which was in good agreement with the analytical results shown in Fig. 1. After four feedings, $20.8\pm0.9$ mM acetate and $15.5\pm0.4$ mM methane were formed from $20.3\pm0.5$ mM propionate. Due to cell aggregation, it was not possible to measure optical densities precisely. Therefore, protein concentration was determined as an alternative parameter for growth. However, in the cultures with aggregate formation, even withdrawal of homogeneous samples was difficult. Thus, the protein curve was not as smooth as the curves for methane and acetate (Fig. 1). Nevertheless, the increase of protein concentration revealed a typical exponential behavior over time, resulting in a doubling time of the enrichment culture of 11 days, which corresponded to a growth rate $\mu$ of 0.062 day$^{-1}$.

Propionate degradation and methane formation rates—influence of acetate

Anaerobic propionate oxidation was coupled with hydrogen formation but proceeded only at low hydrogen partial pressure and thus was dependent on hydrogenotrophic methanogens in our enrichment culture. Figure 2a shows propionate oxidation and methane formation rates during the successive growth phases. Both rates were highest in the third growth phase with maximum values of 0.76 and 0.57 mmoll$^{-1}$day$^{-1}$, respectively, and matched exactly with propionate degradation and methane production rates as deductable from Eqs. (1) and (3) (0.75 mol methane produced from 1 mol propionate oxidized). Specific propionate degradation and methane formation rates are shown in Fig. 2b. To obtain the specific rates, total protein concentration was attributed to propionate degraders and methanogens by hybridizing the mixed culture with 16S rRNA-based oligonucloetide probes targeting MPOB1-related propionate degraders and Arc915-related

methanogens. As a reference, an unspecific staining of all organisms with DAPI was performed and the results were expressed as "biovolume fraction" (Fig. 6). As can be seen
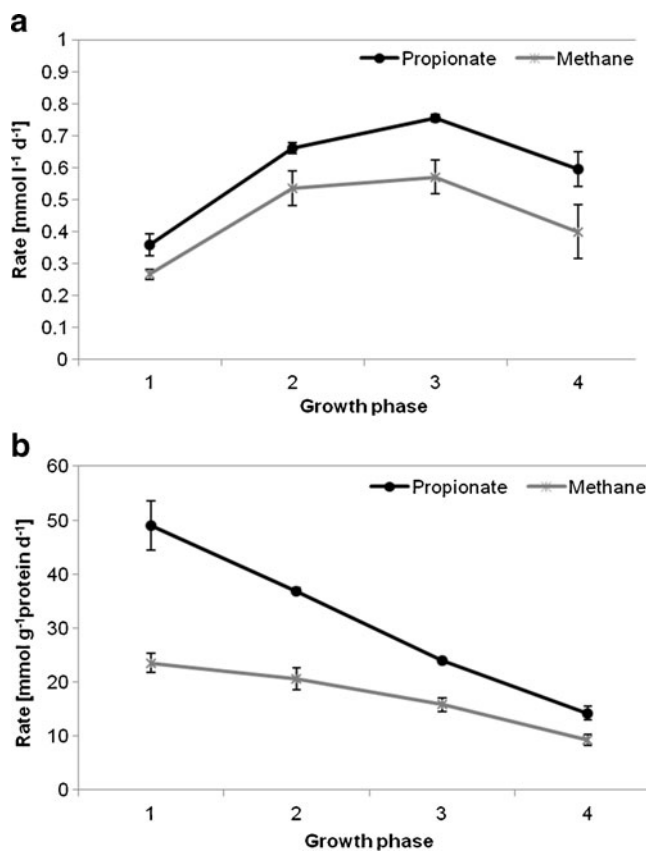


Fig. 2 Propionate oxidation and methane formation rates (Fig. 2a) as well as specific propionate oxidation and methane formation rates (Fig. 2b) during the four growth phases after repeated propionate feeding. Specific rates were obtained by taking the respective total protein concentration of all bacteria from Fig. 1 and calculating the protein content of the propionate degraders and of the methanogens according to their biovolume fraction in phases 1–4 after MPOB1- and Arc915-specific labeling (Fig. 6)

in Fig. 2b, the specific propionate oxidation and methane formation rates decreased linearly with incubation time. The maximum specific propionate oxidation and methane formation rates resulted during the first feeding and were 49 and 23 mmol mg$^{-1}$ day$^{-1}$, respectively. Decreasing specific propionate oxidation and methane formation rates after repeated propionate feedings may indicate an inhibition of syntrophic propionate degradation in the enrichment culture. To test whether the accumulating acetate inhibited propionate oxidation, 5, 10, 15, and 20 mM acetate were supplemented and the propionate degradation rates with initial propionate concentrations of 5 mM were measured (Fig. 3), simulating the conditions during the four successive feeding cycles of Fig. 1. Without external acetate addition, 0.32 mmol l$^{-1}$ day$^{-1}$ propionate was oxidized, which corresponded well with the results shown in Fig. 2a, where the propionate oxidation rate in phase 1 was 0.35 mmol l$^{-1}$ day$^{-1}$ (= 100 %). When 5 mM acetate was supplied together with 5 mM propionate, the propionate oxidation rate decreased to 77.7 % and in the presence of 10, 15, and 20 mM acetate to 60.7, 57.9, and 52.9 %, respectively (Fig. 3), indicating an increasing end-product inhibition.

Formate as an alternative electron carrier

Hydrogen and/or formate may serve for interspecies electron flow between syntrophic propionate degraders and methanogens. Since both partners might express formate dehydrogenase, formate might be produced from NADH + H$^+$ at a concentration of less than 0.01 mM and a redox potential of < −290 mV (Sieber et al. 2012) or from H$_2$ and CO$_2$. Vice versa it might be degraded by both organisms. To test whether formate was released by the propionate oxidizers and consumed by the methanogens in the syntrophic enrichment culture, batch tests with H$_2$/CO$_2$, formate, and propionate in the absence and presence of the methanogenic inhibitor BESA were performed. Methane formation (Fig. 4a) and intermediary-released formate (Fig. 4b) were analyzed. When

H$_2$/CO$_2$ was supplied for the mixed culture, methane and significant amounts of formate were the reaction products. Whereas methane must have been generated by the methanogens, formate might have been generated by both, methanogens and/or propionate degraders. In the presence of H$_2$/CO$_2$ and propionate, BESA-inhibited assays did not produce methane but released some formate produced by the methanogens, propionate degraders, or both. In non-inhibited cultures, hydrogen and CO$_2$ from cleavage of externally added formate was converted to methane by the methanogens at a rate of 0.042 mmol l$^{-1}$ day$^{-1}$, which was six times lower than the methane production rate from H$_2$/CO$_2$ (0.26 mmol l$^{-1}$ day$^{-1}$). In an assay with propionate, the methane formation rate from the degradation products H$_2$ and CO$_2$ (aceticlastic methanogens were not present in the mixed culture) was only 0.037 mmol l$^{-1}$ day$^{-1}$ due to slow propionate degradation. No formate was detectable as a product or intermediate under these conditions. Some formate was, however, produced from propionate when methanogenesis was inhibited completely by BESA (Fig. 4a, b). Whether the propionate degraders generated the formate already or whether they excreted H$_2$/CO$_2$ and the formate was formed by the methanogens via formate dehydrogenase could not clearly be distinguished. However, it is probable that formate was generated exclusively or predominantly by the methanogens since they were able to form a similar amount of formate from H$_2$/CO$_2$ during complete
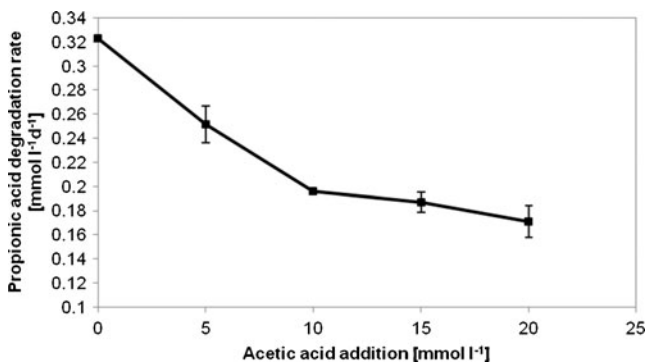


Fig. 3 Inhibiting effect of acetic acid on propionate degradation. The initial propionate concentration was 5 mM in each assay. Different acetate concentrations were added to each assay
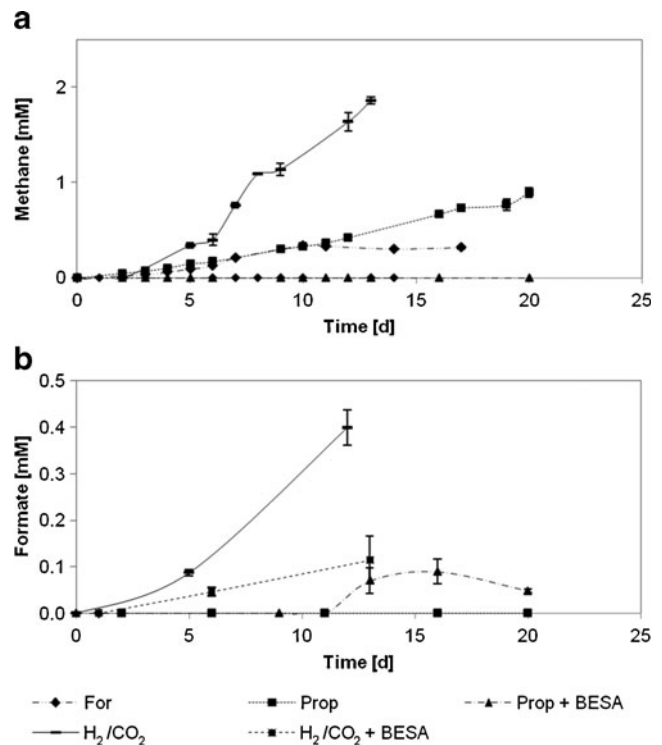


Fig. 4 Methane (a) and formate (b) production by the syntrophic culture after addition of respective substrates ± BESA as an inhibiting agent for methanogens; *For* formate, *Prop* propionate, *BESA* bromo-ethane sulfonic acid

inhibition of methanogenesis with BESA (Fig. 4a, b). A direct proof of interspecies hydrogen transfer during propionate oxidation with and without BESA failed due to a too-high detection limit of hydrogen by the available gas chromatograph of 128 Pa and presumably its conversion to formate only at > 128 Pa hydrogen partial pressure when methanogenesis was inhibited by BESA. No methane formation was observed after addition of BESA to all assays, indicating the successful inhibition of methanogenesis (Fig. 4a).

Species distribution in aggregates

To visualize syntrophic propionate degraders and methanogens in naturally occurring aggregates during propionate oxidation, specific 16S rRNA-based nucleotide probes with Cy3 label (orange fluorescence) for Arc915-related methanogens and FAM label (green fluorescence) for MPOB1-related propionate oxidizers were hybridized with the respective parent DNA, and microphotographs were taken during successive growth phases (Fig. 5). The total bacterial population was visualized by counterstaining with DAPI (Fig. 5, left row). Directly after inoculation in phase 0 and after only 13 days of incubation in growth phase 1, single cells could be seen, which aggregated and formed flocs in growth phase 2 to 4. The aggregates were visualized by "3D microscopic images" obtained from a series of 2D microphotographs representing different levels of cross-section through the aggregates after conversion with the AxioVision software and "extended image definition". The growth of aggregates during the different growth phases can be seen in Fig. 5a–j. Initially, single-cell suspensions were dominant, which were succeeded by small aggregates and finally by big floc-like aggregates. Aggregate disintegration in growth phases 3 and 4 is visible in Fig. 5h, j. Flocs contained propionate degraders aside from methanogens. Some micro-colonies that only contained propionate degraders were also present (data not shown), but their distribution in aggregates was not homogenous or predictable.

From DAPI and FISH images of aggregates in samples taken during different growth phases, the proportion of each syntrophic partner group was calculated by using the *daime* software for digital image analysis. The biovolume fraction of propionate degraders that hybridized with KOP1- and MPOB1-specific probes, of methanogenic bacteria that hybridized with the Arc915-specific probe, and of prokaryotic organisms that hybridized with the *Bacteria*-specific Eub338 probe was determined and expressed as percentage of the total population (Fig. 6). During the consecutive feeding phases, the proportion of methanogenic bacteria remained relatively constant, representing approximately 52 % of the total population. The numbers of both examined propionate-degrading groups of acetogens were increasing within successive feedings. The KOP1-related biovolume fraction increased from initially 7 to 29 % after the fourth feeding with propionate, whereas the

MPOB1-related biovolume fraction that includes also other propionate degraders (*S. fumaroxidans*) aside of KOP1 organisms increased with time from 12 to 50 % of the total biovolume.

Interspecies distances and aggregates growth

The dimensions of flocs containing MPOB1-related propionate degraders and Arc915-related methanogens after successive propionate feedings and the distances between organisms were manually determined from the "3D" microscopic images (Fig. 7). It can clearly be seen that interspecies distances between propionate degraders and methanogens were decreasing with incubation time. Initially, the average distance of a single bacterium from each other was 5.3 μm (phase 0). The interspecies distance decreased to 1.56 μm after the first propionate feeding (phase 1), presumably due to aggregation. After the second, third, and fourth feeding, the interspecies distance decreased further to 0.44, 0.53, and 0.29 μm, respectively. Decreasing interspecies distances were reversely correlated with an increasing dimension of the aggregates in $x$, $y$, and $z$ direction. The $x$ parameter (broadness) was taken as a representative size value of the multidimensional aggregate and was plotted against growth (Fig. 7). The size of the aggregates increased from 18.8 to 54.3 μm after four feedings. There was almost no increase of the aggregate size during incubation after the fourth feeding, indicating a decreasing stability of the aggregates with a high tendency for disintegration (e.g., Fig. 5h, j).

With Fick's diffusion law (Eq. 4), the $H_2$ flux ($J_{H_2}$) from producers to consumers could be calculated. The surface area of the $H_2$-producing, propionate-degrading organisms ($A_{PA}$) was calculated from the surface of single organisms (1.58 μm$^2$) and multiplied by the cell number per milliliter, the hydrogen diffusion constant in water ($D_{H_2}$) at 37 °C was $8.27 \times 10^{-5}$ cm$^2$ s$^{-1}$, and the difference of the hydrogen concentration between hydrogen producer ($C_{PA}$ of 9.34 Pa) and hydrogen consumer ($C_{H_2}$ of 0.32 Pa) was set constant at a value of 9.02 Pa. The Henry constant for solubility of $H_2$ in water at 37 °C was 9.57 nmol l$^{-1}$ Pa$^{-1}$. The interspecies distance (μm) between the two considered organisms ($d_{PAH_2}$) was experimentally determined during the respective growth phases. Table 1 shows the calculated maximum possible hydrogen fluxes $J_{H_2}$ during increasing incubation time. The hydrogen flux depended on the hydrogen concentration gradient between producer and consumer and on the interspecies distance. In phase 1, the maximum possible hydrogen flux was 1.1 nmol ml$^{-1}$ min$^{-1}$. It increased with decreasing interspecies distances to a maximal value in phase 4 of 10.3 nmol ml$^{-1}$ min$^{-1}$ (Table 1). The hydrogen formation rates from propionate oxidation and the hydrogen consumption rates for methane production were considerably lower than the calculated maximum possible

**Fig. 5** Microphotographs of the propionate-degrading enrichment culture. *Left row*—DAPI staining of all bacteria and *right row*—hybridization with Cy3-labeled Arc915 and FAM-labeled MPOB1 oligonucleotide probe of the same images showing single bacteria after inoculation in phase 0 (**a**, **b**), loose floc formation in phase 1 (**c**, **d**), aggregate growth in phases **2** and **3**, respectively (**e**, **f** and **g**, **h**, respectively), and beginning aggregate disintegration in phase 4 (**i**, **j**)
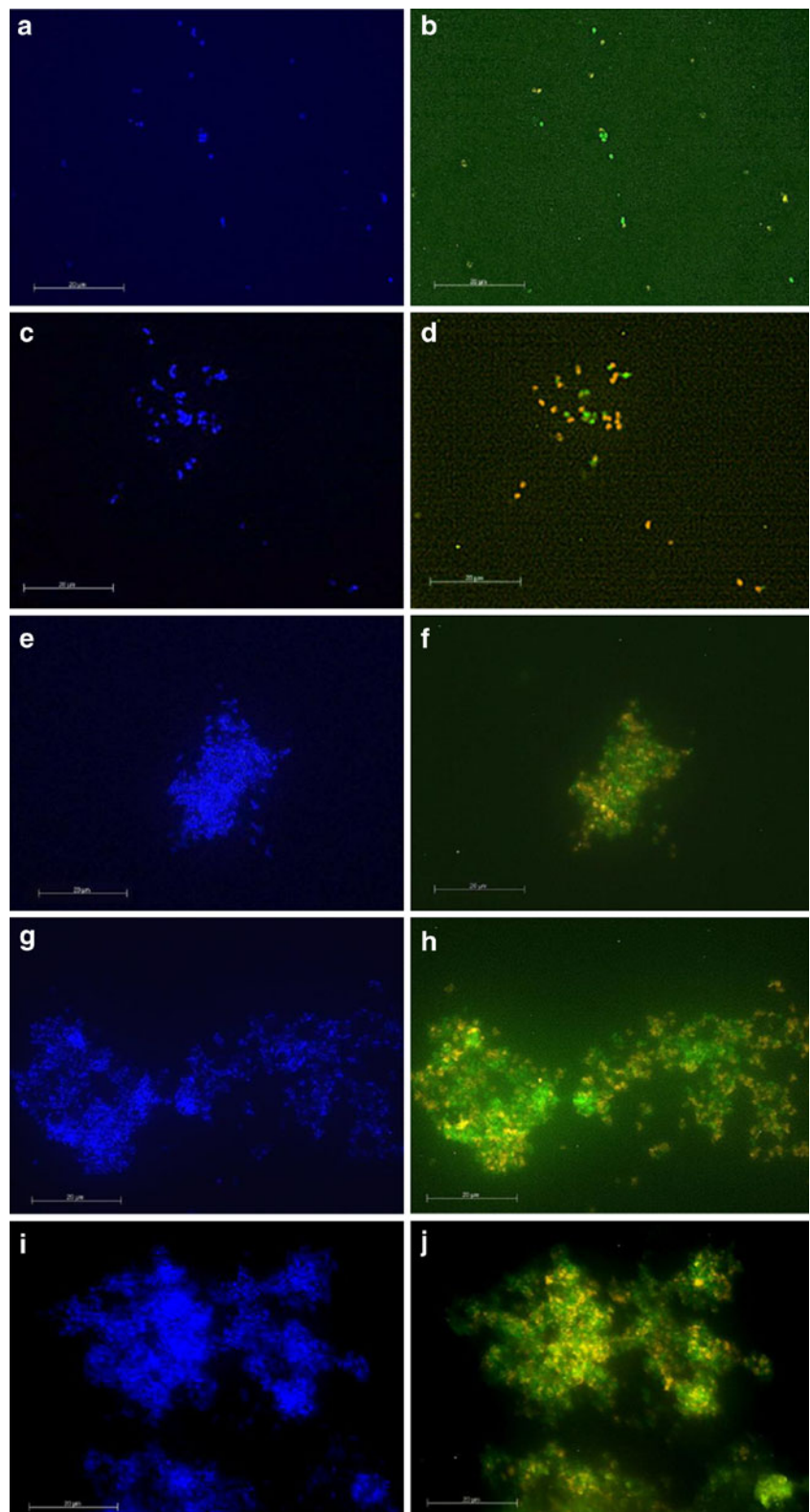


hydrogen flux. Hydrogen production and hydrogen consumption rates were in the same range, first increasing with floc formation and then decreasing when flocs began to decay (Table 1).

## Discussion

The propionate-degrading enrichment culture multiplied with a growth rate of $\mu = 0.062$ day$^{-1}$ (Fig. 1) as
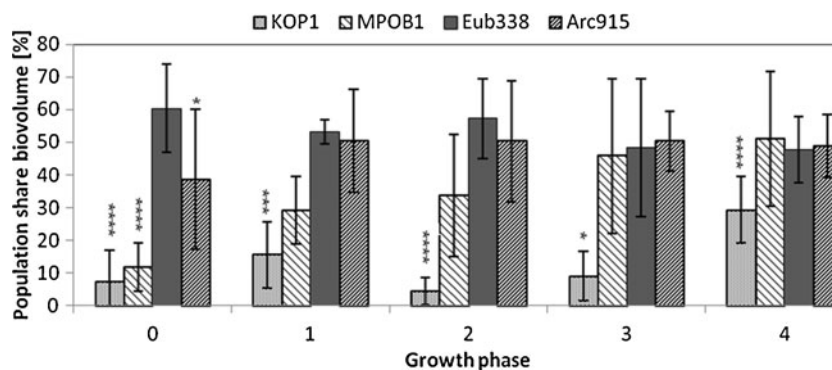
Fig. 6 Population analysis of the enriched propionate-degrading culture. The biovolume fractions were estimated as percentage of organisms that hybridized with the mentioned 16S rRNA-targeted oligonucleotide probes compared to the total biovolume determined with DAPI staining. Whereas the probe KOP1 detected only *S. pfennigii*-related organisms the probe MPOB1 gave a signal for *S. fumaroxidans*-related and *S. pfennigii*-related propionate oxidizers. The probe Eub338 detected almost all microorganisms belonging to the domain *Bacteria* and the probe Arc915 all microorganisms belonging to the domain *Archaea*. According to two-way ANOVA, the biovolume fraction determined for a certain organism group with results determined for all other species was $p=0.03$ for KOP1, $p=0.007$ for MPOB1, $p=0.08$ for Eub338, $p=0.01$ for Arc915; the same test—all measurements vs. Eub338 (as a control data set); $*p<0.05$; $***p<0.001$; $****p<0.0001$

determined from the increase of the total protein during exponential growth. According to data from literature (Table 2), the growth rates obtained from different pure cultures of mesophilic syntrophic propionate degraders in co-culture with hydrogenotrophic methanogens were in the range from 0.066 to 0.19 $day^{-1}$. The growth rates of syntrophic propionate degraders in axenic cultures in the presence of sulfate were still much lower than those of the sulfate reducers when grown in pure culture in the presence of sulfate. This might mean that syntrophic acetogenic bacteria were possibly suppressed by sulfate reducers in sulfate-rich ecosystems.

Our propionate-degrading enrichment culture could oxidize propionate with a rate of 0.76 $mmol l^{-1} day^{-1}$ (Fig. 2a). This rate was higher than that for pure cultures (Table 2) but one order of magnitude lower than the rate of propionate oxidation in the biowaste CSTR full-scale mesophilic digester for treatment of a biowaste suspension from the same origin (8.10 $mmol l^{-1} day^{-1}$; Gallert and Winter 2008). It was two orders of magnitude lower than the rate of propionate oxidation by mesophilic sludge of a lab-scale digester, also treating a biowaste suspension (83.2 $mmol l^{-1} day^{-1}$; Gallert et al. 2003). Since conversion rates in general depend on biomass concentration, it is necessary to relate degradation to active biomass, volatile suspended solids (VSS), or protein. To allow comparison of our results with data from literature, we calculated specific degradation rates from the total protein content under the assumption that 50 % of the dry matter of bacteria would be protein. Thus, the specific propionate oxidation rate of 49 mmol (mg protein)$^{-1}$ day$^{-1}$ (Fig. 2b) of our enrichment culture corresponding to 24.8 mmol (mg VSS)$^{-1}$ day$^{-1}$. This propionate oxidation rate is much higher than the propionate oxidation rate of 1.1 mmol (g VSS)$^{-1}$ day$^{-1}$ measured in the sludge from an anaerobic hybrid reactor (Lens et al. 1996) or of 9.14 mmol (mg VSS)$^{-1}$ day$^{-1}$ measured in granular sludge (Schmidt and Ahring 1995).

The degradation of propionate was inhibited by more than 50 % if acetate accumulated to 20 mM (Fig. 3). Similar results were obtained by Mawson et al. (1991) who reported a 50-% inhibition of propionate oxidation in the presence of 33 mM acetate. This was not caused by a pH change since the pH of the medium was sufficiently buffered.

Hydrogen or formate could be electron carriers from producers (acetogenic bacteria) to consumers (methanogenic bacteria), and the efficiency of electron transfer depends on interspecies distances. Possibilities to reduce transfer distances in liquid suspensions include either the use of artificially concentrated, dense cultures, or autoaggregated flocs, granules, or pellets. Floc formation of our enrichment culture from a biowaste digester during syntrophic propionate degradation
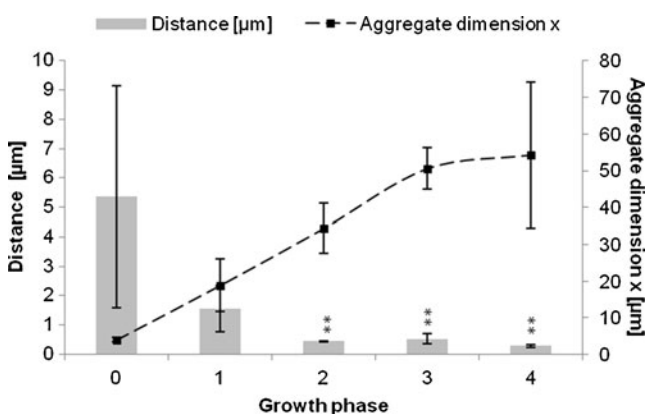


Fig. 7 Increasing aggregate dimensions versus decreasing distances between propionate-degrading and methane-producing bacteria during growth phases 0–4. $**p<0.01$, one-way ANOVA (distances between organisms in phases 2–4 vs. distances in phase 0); the one-way analysis of variance for the distance measurements within several growth phases gave the value of $p=0.0009$

**Table 1** Comparison of hydrogen formation rates, hydrogen consumption rates, and the hydrogen flux from the propionate oxidizers to the methanogens in the syntrophic propionate-degrading culture

| Growth phase (culture age) | Hydrogen flux $J_{H_2}$[a] $[nmol\,ml^{-1}\,min^{-1}]$ | Hydrogen formation rate[b] $[nmol\,ml^{-1}\,min^{-1}]$ | Hydrogen consumption rate[c] $[nmol\,ml^{-1}\,min^{-1}]$ |
|---|---|---|---|
| 1 (13 days) | 1.10 | 0.746±0.070 | 0.741±0.030 |
| 2 (22 days) | 4.48 | 1.375±0.021 | 1.486±0.280 |
| 3 (29 days) | 5.06 | 1.572±0.017 | 1.583±0.237 |
| 4 (42 days) | 10.30 | 1.239±0.112 | 1.111±0.208 |

[a] $J_{H_2}$ was calculated according to Fick's diffusion law; cell numbers of MPOB1-related propionate degraders in phase 1 were $5.05 \times 10^7\ ml^{-1}$, in phase 2 $5.83 \times 10^7\ ml^{-1}$, in phase 3 $7.91 \times 10^7\ ml^{-1}$, and in phase 4 $8.82 \times 10^7\ ml^{-1}$; cell numbers were calculated from the total cell number and percentage of MPOB1-related propionate degraders in each growth phase from Fig. 5

[b] The hydrogen formation rate was calculated from the propionate oxidation rate assuming that 3 mol of $H_2$ were produced per mole of propionate (data from Fig. 2a)

[c] The hydrogen consumption rate was calculated from the methane formation rate assuming that 4 mol of $H_2$ were consumed per mol of methane (data from Fig. 2a)

was observed (Fig. 5c–j), and an increasing size of the flocs up to 54 μm was determined (Fig. 7). Cluster formation of fatty acid-oxidizing acetogenic bacteria and $H_2$-oxidizing methanogenic bacteria seems to facilitate hydrogen transfer (Conrad et al. 1986). Microscopic observations of flocs in syntrophic methanogenic cultures revealed the close neighborhood of acetogens and methanogens, allowing conclusions on the kinetics of interspecies electron transfer within the flocs (Thiele et al. 1988). The close neighborhood of propionate degraders and of methanogens in our floc-forming enrichment culture can be seen in Fig. 5c–j. The advantage of aggregation in syntrophic populations that degraded volatile fatty acids via interspecies hydrogen transfer was also investigated in sludge granules. With propionate as substrate, a 50-% higher $H_2$ consumption, measured as specific methanogenic activity, and a 20-% higher propionate oxidation were reported for intact granular sludge as compared to bacterial suspensions after disintegration of the granules (Shi-yi and Jian 1992; Schmidt and Ahring 1995). In experiments with co-cultures of thermophilic *Pelotomaculum thermopropionicum* and *Methanobacterium thermoautotrophicum*, co-aggregation apparently depended on the type of substrate. With thermodynamically unfavorable propionate, a large fraction of cells co-aggregated, whereas a relatively small fraction of cells co-aggregated with ethanol or *1*-propanol as substrates (Ishii et al. 2005). In suspended propionate-degrading syntrophic cultures, one option to decrease interspecies distances is to increase the proportion of hydrogenotrophic methanogens for enhanced mass transfer of metabolites (Amani et al. 2012).

The methanogens in our propionate-degrading enrichment culture were able to produce methane from $H_2/CO_2$ and at a much lower rate from formate (Fig. 4a). Vice versa, formate was generated by methanogens when $H_2/CO_2$ was introduced into the gas phase and thus surplus hydrogen was available (Fig. 4b). Some formate (maximally 0.09 mM) was also excreted by this culture in the presence of propionate when hydrogenothrophic methanogenesis was completely inhibited. Formate formation from $H_2/CO_2$ would only require an active formate dehydrogenase and might stem from the methanogens, the propionate degraders, or both. With fumarate as an electron acceptor, Dong and Stams (1995) reported a minimal concentration of 0.024 mM formate that was generated by the MPOBs from propionate. In our non-BESA-inhibited batch assay with propionate, no formate was detected. In the literature, a controversial discussion is documented about the requirement or participation of formate, hydrogen, or both for electron interspecies transfer. Some authors state that both are equally important for syntrophic bacteria (Batstone et al. 2006; Schink 1997) or that formate may be more significant (de Bok et al. 2004) with fluxes 100 times higher than those for hydrogen in a co-culture of MPOBs and *Methanospirillum hungatei* (Dong and Stams 1995). Formate as an electron shuttle component may not be significant in suspensions of disintegrated thermophilic granules (Schmidt and Ahring 1993) or for mesophilic granular sludge (Schmidt and Ahring 1995),

The spatial distribution of propionate degraders and methanogens in our syntrophic enrichment culture was visualized with fluorescence in situ hybridization using specific 16S rRNA-targeted oligonucleotides labeled with FAM (propionate degraders) or Cy3 (methanogenic bacteria). The species of both trophic groups of bacteria in the flocs were almost randomly distributed with the formation of only very little micro-colonies. In order to quantify population changes during the different growth phases, the *daime* software for digital image analysis in microbial ecology was implemented (Daims et al. 2006) and biovolume fractions were determined. The total biovolume was obtained from DAPI-stained preparations, whereas the biovolume fractions of the propionate-degrading acetogens and the methane-forming archaea were determined with group-specific 16S rRNA-based oligonucleotide probes. Although DAPI has its limitations for such kind of evaluation (Nielsen et al. 2009), using it as a basis for the description of population fluctuations at each growth phase gave a sufficiently reliable "external" marker for changes of the ratio of propionate degraders and methanogens. The relative abundance of methanogens that hybridized with the specific 16S rRNA-targeted oligonucleotide probe Arc915 remained almost constant over the whole period of 42 days with four propionate feedings and accounted for approximately 52 % of the total biovolume in relation to

**Table 2** Comparison of growth rates of pure cultures of propionate-degrading microorganisms

| Propionate degrader | Syntrophic partner/co-substrate | Growth rate, $\mu$ [day$^{-1}$] | Reference |
|---|---|---|---|
| Pure cultures of syntrophic propionate-degrading bacteria | | | |
| *Syntrophobacter fumaroxidans* | *Methanospirillum hungatei* | 0.17 | Harmsen et al. 1998 |
| | Fumarate (no propionate) | 0.09 | |
| | Sulfate | 0.024 | Van Kuijk and Stams 1995; Harmsen et al. 1998 |
| *Syntrophobacter pfennigii* | *Methanospirillum hungatei* | 0.066[a] | Wallrabenstein et al. 1995 |
| | Sulfate | 0.069[a] | |
| *Syntrophobacter sulphatireducens* | *Methanospirillum hungatei* | 0.12 | Chen et al. 2005 |
| *Syntrophobacter wolinii* | *Methanospirillum hungatei* and *Desulfovibrio* | 0.10[a] | Boone and Bryant 1980 |
| | Sulfate and *Desulfovibrio* | 0.19[a] | |
| | Sulfate | 0.062 | Wallrabenstein et al. 1994 |
| *Smithella propionica* | *Methanospirillum hungatei* | n.d.[b] | Liu et al. 1999 |
| *Pelotomaculum schinkii* | *Methanospirillum hungatei*; *Methanobacterium formicium* | 0.099[a] | de Bok et al. 2005 |
| *Pelotomaculum thermopropionicum* | *Methanothermobacter thermoautotrophicus* | 0.19 | Imachi et al. 2000; Imachi et al. 2002 |
| | Pyruvate (no propionate) | 1.65 | |
| *Desulfotomaculum thermocisternum* | Hydrogenotrophic methane bacterium; sulfate | n.d.[b] | Nilsen et al. 1996 |
| *Desulfotomaculum thermobenzoicum* subsp. *thermosyntrophicum* | *Methanobacterium thermoautotrophicum* | 0.12 | Plugge et al. 2002 |
| | Pyruvate (no propionate ) | 0.33 | |
| | Sulfate | 0.099 | |
| Pure cultures of selected sulfate-reducing propionate-degrading bacteria | | | |
| *Desulfobulbus propionicus* | Sulfate | 0.89 | Stams et al. 1984 |
| | Sulfate | 1.66[a] | Widdel and Pfennig 1982 |
| *Desulfobulbus elongatus* | Sulfate | 1.39 | Samain et al. 1984 |
| Strain PW | *Methanobacterium formicium* | 0.14[a] | Wu et al. 1992 |
| | Sulfate | 0.23[a] | |

[a] Conversion of $t_d$ into $\mu$ using $\mu = \ln 2/t_d$

[b] Not determined

unspecific DAPI staining (Fig. 6). Comparable results were reported for granular sludge fed with propionate, where the archaeal population remained constant at 55 % over 12 weeks (Harmsen et al. 1996). The biovolume fraction of propionate degraders in our enrichment culture, which hybridized with the 16S rRNA-targeted oligonucleotide probe KOP1 (*S. pfennigii*-related organisms) and MPOB1 (*S. fumaroxidans*-related organisms, including also *S. pfennigii*-related organisms), increased with time during the different growth phases. The biovolume fraction of MPOB-like propionate degraders accounted for 50 % after 42 days and was almost identical with the percentage value for the biovolume fraction that was obtained after hybridization with the universal EUB-probe (Fig. 6). Resilience and resistance of both methanogens and syntrophic propionate degraders must guarantee a stable metabolic function over time for survival despite disturbances.

Floc or aggregate formation was a possibility to decrease the interbacterial distance, which was necessary for the fast transfer of metabolites. In the literature, interspecies distances of 12.4 μm in co-cultures of *S. fumaroxidans* and

*M. hungatei* (Stams and Dong 1995), of 4 μm in mesophilic granular sludge between hydrogen-producing and hydrogen-consuming bacteria (Stams et al. 1989), of 2–3 μm in intact mesophilic sludge granules (Schmidt and Ahring 1995), or of 2.3 μm in aggregates of thermophilic *P. thermopropionicum* and *M. thermoautotrophicum* (Ishii et al. 2005) were reported. In our experiments, the interspecies distances decreased from 5.3 μm in the cell suspension directly after inoculation to 1.56 μm in phase 1, where small flocs were dominant, to 0.29 μm in phase 4 with mainly large flocs (Fig. 7). According to Fick's diffusion law (Eq. 4), an inverse relationship between syntrophic distance and hydrogen flux can be seen. A low spatial distance with a high diffusion rate would allow the maintenance of a low hydrogen partial pressure and enhance syntrophic propionate degradation. Calculation of the hydrogen concentrations according to Eq. 5 gave minimum $H_2$ concentrations of 0.32 Pa for the methanogens and maximum $H_2$ concentrations of 9.34 Pa for the propionate oxidizers delivering a maximum possible $C_{PA} - C_{H_2}$ value. According to de Bok et al. (2004), the highest $H_2$ level formed

by *S. fumaroxidans* was 6.8 Pa and the lowest $H_2$ level reached by *M. hungatei* was 2 Pa. In similar experiments of Scholten and Conrad (2000) with a syntrophic co-culture of *S. fumaroxidans* and *M. hungatei*, maximum $H_2$ concentrations of 9 Pa and minimum $H_2$ concentrations of 0.8 Pa, respectively, were measured. These values were in accordance with those calculated for our co-culture. The maximum possible hydrogen flux $J_{H_2}$ in the successive growth phases increased with decreasing interspecies distances. In phase 1, the maximum possible $J_{H_2}$ was $1.1 \, nmol \, H_2 \, ml^{-1} min^{-1}$, which increased to $10.3 \, nmol \, H_2 \, ml^{-1} min^{-1}$ in phase 4 (Table 1). A $H_2$ flux of $1.1 \, nmol \, H_2 \, ml^{-1} min^{-1}$ in co-cultures of the propionate-degrading strain MPOB and *M. hungatei* was reported (Stams and Dong 1995). A $H_2$ flux of $5.38 \, nmol \, H_2 \, ml^{-1} min^{-1}$ in co-cultures of *P. thermopropionicum* and *M. thermoautotrophicus* can be calculated from the data of Ishii et al. (2005).

Simulation experiments for syntrophic degradation with hydrogen transfer resulted in the co-location of hydrogen producers and hydrogen consumers caused by the high uptake rates of hydrogen consumers rather than the sensitivity of hydrogen producers to hydrogen inhibition (Batstone et al. 2006). Results with our enrichment culture indicated that methanogens and syntrophic propionate degraders "find each other" after inoculation and form aggregates. By lowering the interspecies distance, the hydrogen flux from the hydrogen producer to the hydrogen consumer apparently did not limit the overall syntrophic interaction.

# References

Amani T, Nosrati M, Mousavi SM (2012) Response surface methodology analysis of anaerobic syntrophic degradation of volatile fatty acids in an upflow anaerobic sludge bed reactor inoculated with enriched cultures. Biotechnol Bioproc Eng 17:133–144

Amann RI, Binder BJ, Olson RJ, Chisholm SW, Devereux R, Stahl DA (1990) Combination of 16S rRNA-targeted oligonucleotide probes with flow cytometry for analyzing mixed microbial population. Appl Environ Microbiol 56:1919–1925

Batstone DJ, Picioreanu C, van Loosdrecht MCM (2006) Multidimensional modeling to investigate interspecies hydrogen transfer in anaerobic biofilms. Wat Res 40:3099–3108

Bleicher K, Winter J (1994) Formate production and utilization by methanogens and by sewage sludge consortia—interference with the concept of interspecies formate transfer. Appl Microbiol Biotechnol 40:910–915

Boone DR, Bryant MP (1980) Propionate-degrading bacterium, *Syntrophobacter wolinii* sp. nov. gen. nov., from methanogenic ecosystems. Appl Environ Microbiol 40:626–632

Bryant MP, Wolin EA, Wolin MJ, Wolfe RS (1967) "*Methanobacillus omelanskii*", a symbiotic association of two species of bacteria. Arch Microbiol 59:20–31

Chen S, Liu X, Dong X (2005) *Syntrophobacter sulfatireducens* sp. nov., a novel syntrophic, propionate-oxidizing bacterium isolated from UASB reactors. Int J Syst Evol Microbiol 55:1319–1324

Conrad R, Schink B, Phelps TJ (1986) Thermodynamics of $H_2$-consuming and $H_2$-producing metabolic reactions in diverse methanogenic environments under in situ conditions. FEMS Microbiol Ecol 38:353–360

Daims H, Lücker S, Wagner M (2006) *daime*, a novel image analysis program for microbial ecology and biofilm research. Environ Microbiol 8:200–213

De Bok FAM, Stams AJM, Dijkema C, Boone DR (2001) Pathway of propionate oxidation by syntrophic culture of *Smithella propionica* and *Methanospirillum hungatei*. Appl Environ Microbiol 67:1800–1804

De Bok FAM, Plugge CM, Stams AJM (2004) Interspecies electron transfer in methanogenic propionate degrading consortia. Water Res 38:1368–1375

de Bok FAM, Harmsen HJM, Plugge CM, de Vries MC, Akkermans DL, de Vos WM, Stams AJM (2005) The first true obligately syntrophic propionate-oxidizing bacterium, *Pelotomaculum schinkii* sp. nov., co-cultured with *Methanospirillum hungatei*, and emended description of the genus *Pelotomaculum*. Int J Syst Evol Microbiol 55:1697–1703

Dong X, Stams AJM (1995) Evidence for $H_2$ and formate formation during syntrophic butyrate and propionate degradation. Anaerobe 1:35–39

Dwyer DF, Weeg-Aerssens E, Shelton DR, Tiedje JM (1988) Bioenergetic conditions of butyrate metabolism by a syntrophic, anaerobic bacterium in coculture with hydrogen-oxidizing methanogenic and sulfidogenic bacteria. Appl Environ Microbiol 54:1354–4359

Felchner-Zwirello M, Winter J, Gallert C (2012) Mass spectrometric identification of $^{13}C$- labeled metabolites during anaerobic propionic acid oxidation. Chem Biodiv 9:376–384

Gallert C, Winter J (2005) Bacterial metabolism in wastewater treatment systems. In: Jördening HJ, Winter J (eds) Environmental biotechnology—concept and applications. Wiley, Weinheim, pp 1–48

Gallert C, Winter J (2008) Propionic acid accumulation and degradation during restart of a full-scale anaerobic biowaste digester. Bioresour Technol 99:170–178

Gallert C, Henning A, Winter J (2003) Scale-up of anaerobic digestion of the biowaste fraction from domestic wastes. Wat Res 37:1433–1441

Gerardi MH (2003) The microbiology of anaerobic digesters. Wiley, New Jersey

Gujer W, Zehnder AJB (1983) Conversion processes in anaerobic digestion. Wat Sci Technol 15:127–167

Harmsen HJM, Kengen HMP, Akkermans ADL, Stams AJM (1995) Phylogenetic analysis of two syntrophic propionate-oxidizing bacteria in enrichment cultures. Syst Appl Microbiol 18:67–73

Harmsen HJM, Akkermans ADL, Stams AJM, De Vos WM (1996) Population dynamics of propionate-oxidizing bacteria under methanogenic and sulfidogenic conditions in anaerobic granular sludge. Appl Environ Microbiol 62:2163–2168

Harmsen HJM, Van Kuijk BLM, Plugge CM, Akkermans ADL, De Vos WM, Stams AJM (1998) *Syntrophobacter fumaroxidans* sp. nov., a syntrophic propionate-degrading sulfate-reducing bacterium. Int J Syst Bacteriol 48:1383–1387

Imachi H, Sekiguchi Y, Kamagata Y, Ohashi A, Harada H (2000) Cultivation and in situ detection of a thermophilic bacterium capable of oxidizimg propionate in syntrophic association with hydrogenotrophic methanogens in a thermophilic methanogenic granular sludge. Appl Environ Microbiol 66:3608–3615

Imachi H, Sekiguchi Y, Kagamata Y, Hanada S, Ohashi A, Harada H (2002) *Pelotomaculum thermopropionicum* gen. nov., sp. nov., an anaerobic, thermophilic, syntrophic propionate- oxidizing bacterium. Int J Syst Evol Microbiol 52:1729–1735

Inanc B, Matsui S, Ide S (1999) Propionic acid accumulation in anaerobic digestion of carbohydrates: an investigation on the role of hydrogen gas. Wat Sci Tech 40:93–100

Ishii S, Kosaka T, Hori K, Hotta Y, Watanabe K (2005) Coaggregation facilitates interspecies hydrogen transfer between *Pelotomaculum thermopropionicum* and *Methanothermobacter thermoatotrophicus*. Appl Environ Microbiol 71:7838–7845

Lens PNL, O'Flaherty V, Dijkema C, Colleran E, Stams AJM (1996) Propionate degradation by mesophilic anaerobic sludge: degradation pathways and effects of other volatile fatty acids. J Ferment Bioeng 82:387–391

Liu Y, Balkwill DL, Aldrich HC, Drake GR, Boone RD (1999) Characterization of the anaerobic propionate degrading syntrophs *Smithella propionica* gen. nov., sp. nov. and *Syntrophobacter wolinii*. Int J Syst Bacteriol 49:545–556

Lowry OH, Rosenbrough NJ, Farr AL, Randall RJ (1951) Protein measurement with the folin phenol reagent. J Biol Chem 193:265–275

Mawson AJ, Earle RL, Larsen VF (1991) Degradation of acetic and propionic acids in the methane fermentation. Water Res 12:1549–1554

McCarty PL, Smith DP (1986) Anaerobic wastewater treatment. Environ Sci Technol 20:1200–1206

Müller N, Worm P, Schink B, Stams AJM, Plugge CM (2010) Syntrophic butyrate and propionate oxidation processes: from genomes to reaction mechanisms. Environ Microbiol Rep 2:489–499

Nielsen H, Daims H, Lemmer H (2009) FISH handbook for biological wastewater treatment: Identification and quantification of microorganisms in activated sludge and biofilms by FISH. IWA, London

Nilsen RK, Torsvik T, Lien T (1996) *Desulfotomaculum thermocisternum* sp. nov., a sulfate reducer isolated from a hot North Sea oil reservoir. Int J Syst Bacteriol 46:397–402

Plugge CM, Dijkema C, Stams AJM (1993) Acetyl–CoA cleavage pathway in a syntrophic propionate oxidizing bacterium growing on fumarate in the absence of methanogens. Microbiol Lett 110:71–76

Plugge CM, Balk M, Stams AJM (2002) *Desulfotomaculum thermobenzoicum* subsp. *thermosyntrophicum* subsp. nov., a thermophilic, syntrophic, propionate-oxidizing, spore-forming bacterium. Int J Syst Evol Microbiol 52:391–399

Samain E, Dubourguier HC, Albagnac G (1984) Isolation and characterization of *Desulfobulbus elongatus* sp. nov. from a mesophilic industrial digester. Syst Appl Microbiol 5:391–401

Schink B (1992) Syntrophism among prokaryotes. In: Balows A, Trüper HG, Dworkin M, Harder W, Schleifer K-H (eds) The prokaryotes, 3rd edn. Springer, New York, pp 276–299

Schink B (1997) Energetics of syntrophic cooperation in methanogenic degradation. Microbiol Mol Biol Rev 61:262–280

Schmidt JE, Ahring BK (1993) Effects of hydrogen and formate on the degradation of propionate and butyrate in thermophilic granules from an upflow anaerobic sludge blanket reactor. Appl Environ Microbiol 59:2546–2551

Schmidt JE, Ahring BK (1995) Interspecies electron transfer during propionate and butyrate degradation in mesophilic, granular sludge. Appl Environ Microbiol 61:2765–2767

Scholten JCM, Conrad R (2000) Energetics of syntrophic propionate oxidation in defined batch and chemostat cocultures. Appl Environ Microbiol 66:2934–2942

Shin SG, Lee S, Lee C, Hwang K, Hwang S (2010) Qualitative and quantitative assessment of microbial community in batch anaerobic digestion of secondary sludge. Biores Technol 101:9461–9470

Shi-yi L, Jian C (1992) The contribution of interspecies hydrogen transfer to the substrate removal in methanogenesis. Process Biochem 27:285–289

Sieber JR, McInerney MJ, Gunsalus RP (2012) Genomic insights into syntrophy: the paradigm for anaerobic metabolic cooperation. Annu Rev Microbiol 66:429–452

Stahl DA, Amann R (1991) Development and application of nucleic acid probes. In: Stackebrandt E, Goodfellow M (eds) Nucleic acid techniques in bacterial systematics. Wiley, Chichester, pp 205–248

Stams AJM (1994) Metabolic interactions between anaerobic bacteria in methanogenic environments. Antonie Van Leeuwenhoek 66:271–294

Stams AJM, Dong X (1995) Role of formate and hydrogen in the degradation of propionate and butyrate by defined suspended cocultures of acetogenic and methanogenic bacteria. Antonie Van Leeuwenhoek 68:281–284

Stams AJM, Kremer DR, Nicolay K, Weenk G, Hansen AT (1984) Pathway of propionate formation in *Desulfobulbus propionicus*. Arch Microbiol 139:167–173

Stams AJM, Grothenius JTC, Zehnder AJB (1989) Structure–function relationship in granular sludge. In: Hattori T, Ishida Y, Maruyama R, Morita R, Uchida A (eds) Recent advances in microbial ecology. Japan Scientific Societies, Tokyo, pp 440–445

Thauer RK, Jungermann K, Decker K (1977) Energy conservation in chemotrophic anaerobic bacteria. Bacteriol Rev 41:100–180

Thiele JH, Zeikus JG (1988) Control of interspecies electron flow during anaerobic digestion: significance of formate transfer during syntrophic methanogenesis in flocs. Appl Environ Microbiol 54:20–29

Thiele JH, Chartrain M, Zeikus JG (1988) Control of interspecies electron flow during anaerobic digestion: role of floc formation in syntrophic methanogenesis. Appl Environ Microbiol 54:10–19

Van Kuijk BLM, Stams AJM (1995) Sulfate reduction by a syntrophic propionate-oxidizing bacterium. In: Proceedings of the International Meeting on Anaerobic Processes for Bioenergy and Environment, part 5, Copenhagen, 25–27 January 1995

Wallrabenstein C, Hauschild E, Schink B (1994) Pure culture and cytological properties of *Syntrophobacter wolini*. FEMS Microbiol Lett 123:249–254

Wallrabenstein C, Hauschild E, Schink B (1995) *Syntrophobacter pfennigii* sp. nov., new syntrophically propionate-oxidizing anaerobe growing in pure culture with propionate and sulfate. Arch Microbiol 164:346–352

Wang L, Zhou Q, Li FT (2006) Avoiding propionic acid accumulation in the anaerobic process for biohydrogen production. Biomass Bioenergy 30:177–182

Widdel F, Pfennig N (1982) Studies on dissimilatory sulfate-reducing bacteria that decompose fatty acids. II. Incomplete oxidation of propionate by *Desulfobulbus propionicus* gen. nov., sp. nov. Arch Microbiol 131:360–365

Wolin MJ (1975) Interactions between $H_2$-producing and methane-producing species. In: Schlegel HG, Gottschalk G, Pfennig N (eds) Symposium on microbial production and utilization of gases. Goltz, Göttingen, pp 141–150

Wu WM, Jain MK, de Macario EC, Thiele JH, Zeikus JG (1992) Microbial composition and characterization of prevalent methanogens and acetogens isolated from syntrophic methanogenic granules. Appl Microbiol Biotechnol 38:282–290